LA-UR-77-719

CONF-770544--1

TITLE: A Review of Some Past and Present Powder Metallurgy Programs at the Los Alamos Scientific Laboratory

AUTHOR(S): Haskell Sheinberg

SUBMITTED TO: To be presented at unclassified International Symposium on Powder Metallurgy in Honor of P.G. Sobolevsky, May 11-15, 1977 Kiev, USSR

los alamos
scientific laboratory
of the University of California
LOS ALAMOS, NEW MEXICO 87544

An Affirmative Action/Equal Opportunity Employer

MASTER

EB

DISTRIBUTION OF THIS DOCUMENT IS UNLIMITED

Form No. 836
St. No. 2629
1/75

UNITED STATES
ENERGY RESEARCH AND
DEVELOPMENT ADMINISTRATION
CONTRACT W-7405-ENG. 36

A REVIEW OF SOME PAST AND PRESENT POWDER METALLURGY PROGRAMS AT THE LOS ALAMOS SCIENTIFIC LABORATORY

by

Haskell Sheinberg

Presentation at the International
Symposium on Powder Metallurgy
in honor of P.G. Sobolevsky,
May 11-15, 1977, Kiev, USSR

I. Rover Program (Nuclear Rocket Propulsion Engines)

A. Kiwi Reactor Fuel Elements

The Rover Program aimed at the development of a nuclear reactor as a rocket propulsion engine with high specific impulse. The designed ~ 2500K operation of the first reactor of this program demanded a new class of fuel element material, enriched uranium carbide dispersed in a graphite matrix. The reactor contained a vertical stack of four wheel-like structures with pie shaped boxes of fuel plates as shown in Figure 1. Each box contained twenty plates with uranium content varying from 60 to 300-mg uranium/cc, and positioned so as to provide a relatively flat radial neutron distribution. The plates were required to be radiographically sound with a uniform distribution of uranium and a minimum carbon density of 1.70 Mg/m^3.[1]

After exploring the conventional process for fabrication of commercial graphites employing a thermo-plastic pitch binder, we developed a process using a liquid thermosetting resin, furfuryl alcohol as a binder. A mixture of 77.5 wt% -325 mesh graphite flour, 15.0 wt% carbon black, and 7.5 wt% flake graphite was dry blended with fine uranium oxide and then mixed with catalyzed furfuryl alcohol in the amount of 19% of the dry carbon powders plus 50% of the weight of uranium oxide.

We formed 215-mm by 250-mm by 11.4-mm-thick plate blanks by a die compression vacuum molding technique at 7000 psi (48.2-MPa). The plates were heated in a 36 h cycle from 318 to 453 K to partially polymerize the resin, then impregnated with the resin to increase carbon density, and then reheated slowly to 453 K. The plates were

radiographed at this stage to determine uniformity of uranium distribution and to detect flaws. Acceptable plates were heated in 36 h to 1073 K in vacuum. These long heating cycles were required to permit slow evolution of water from polymerization of the condensation type polymer and for gradual removal of volatile products of polymerization to prevent spalling of the plates.

The plates were then heated in an induction furnace in a 3 h heating cycle to ~ 2800 K which converted most of the carbon to graphite and the uranium oxide to uranium carbide.

The plates were machined flat and inspected by radiographic DXT gaging, and the uranium content was determined by radiation absorption and correlated by chemical analysis. The plates were then machined to provide ribbed surfaces to allow hydrogen gas passage between plates.

B. Phoebus Reactors

Figure 2 is a schematic of the more advanced Phoebus II type cyclable nuclear rocket propulsion engines. Liquid hydrogen enters around the nozzle, cooling it. The hydrogen then passes around the reflector and criticality control material and passes upward through the multiple hole enriched uranium loaded graphite core which heats it to an exit gas temperature of ~ 2720 k. The reactor power level was 5000 megawatts.

The Powder Metallurgy Section was responsible for making the uranium loaded fuel elements, the criticality control material, a neutron poison material required at the forward end of the reactor to reduce the neutron flux peak, structural composites for fuel element supports, and heat shields.

1. Fuel Elements

The uranium loaded graphite fuel elements were in the form of hexagons, 19-mm across flats and 1320-mm-long with nineteen 2.5-mm-diam holes for gas passage. The configuration and specifications of these fuel elements were beyond any commercial capabilities and presented a challenging development program for us. These fuel elements were made using the materials and materials processing as previously described except they were formed by extruding the mixture through a very complicated design nozzle to yield the desired shape as shown in Figure 3.

Complete uniformity of powder and binder mixing, ingenuity in nozzle design and extrusion fixturing, rigid control of extrusion rate, and special fixturing for all phases of subsequent processing were necessary to comply with extremely tight specifications assigned to hole diameter and location, and flatness of the long extruded shape, as well as uniformity of uranium distribution.

2. Criticality Control and Poison Plate Material

The criticality control material was in the form of 50-mm-wide by 203-mm-long by 2.5-mm-thick plates which were spirally mounted on externally activated drums. A total of 360 plates were required. Additionally 1.4-mm-thick nineteen hole neutron poison hexagons with the same cross section and hole alignment as the fuel elements were required.[2]

Copper was chosen as the matrix material primarily because of desirable mechanical properties in the 20K-450K operational temperature range and because of its compatability with normal boron carbide which was used as the neutron absorber.

For feasibility studies, we cold pressed 50-mm-square plates at pressures up to 50-tsi (689-MPa) and sintered them at 980°C,

or hot pressed plates at 950°C and 2200 psi (15-MPa). We used 20, 40, and 50 vol% boron carbide concentrations in these feasibility studies, canned the plates in copper and warm rolled the plates to 1.4-mm-thickness. We radiographed the rolled sheet and then machined tensile and multiple hole dimensional stability specimens by electrical discharge machining.

The high loadings of very hard angular boron carbide caused excessive die wear, and during rolling, resulted in void areas behind the particles in the direction of rolling because of poor flow of the soft copper around these particles. Rounding the carbide particles minimized these problems.

The structure and particle size of the raw materials used for most of these pressings are shown in Figure 4 (660522). We used the rounded boron carbide that we made by passing angular powder through a plasma arc for the higher carbide concentrations. Figure 5 (650164) shows radiographs of typical rolled sheet using three different size carbide powders, + 120, -140+200, and -200 mesh. The uniformity of loading was confirmed by chemical analysis.

Tensile specimens made with rounded and angular boron carbide and using coarse and fine copper powder were annealed in hydrogen and tested both at room temperature and at cryogenic 20 K. Test results indicated that regardless of carbide concentration, mechanical properties of sheet made with rounded carbide particles were slightly higher than those made with angular powder. Strength and elongation decreased as carbide loadings increased. Properties of sheet made with fine copper were superior to those made with coarse copper, and cryogenic mechanical properties were considerably superior to those at room temperature.

We cycled eighteen carefully inspected 1.4-mm-thick twenty-hole stability specimens four times between 20 K and 450 K and determined that the hole size, hole location and true position of the holes were stable.

Production hot pressing of the 20 and 40 vol% carbide loaded material was scaled up in size to form 146-mm-wide by 381-mm-long by 11-mm-thick plates without process modification. The graphite die design used for the hot pressing is shown in Figure 6 (659968) and Figure 7 ( ) shows the type of hot press used.

All production runs employed the rounded boron carbide; a -100 +140 mesh fraction was used for the 40 vol% carbide loaded material and a -140+200 mesh fraction was used for the 20 vol% carbide material.

The hot pressed plates were electroplated with 0.25-mm-thick copper and rolled in steel frame enclosures at 700°C to form 4.6-mm-thick copper-boron carbide sheet which was then rolled bare at 700°C to the final thickness. The sheet was then blanked and warm rolled to form the spiral contoured control plates,or electrical discharge machined to form the thin hexagonal poison plates.

3. Structural Composites for Fuel Element Supports

The hot end of the advanced Phoebus type reactors operated at ~ 2900 K and required critical load bearing fuel element supports in this area, and also in cooler areas of the reactor. It was necessary to develop a new class of materials having considerably higher hot strengths and lower creep rates than niobium carbide coated graphite previously used for this application in lower temperature reactors.

We hot pressed and tested a large number of tantalum carbide-graphite, niobium carbide-graphite, and solid solution TaC-NbC-graphite composites; the latter offered a new family of materials having high temperature mechanical and physical properties vastly different than those of the individual carbide-graphite composites. Considerable effort was expended on complete powder characterization, and the effects of powder characteristics and chemistry on properties; especially deformation at high temperature of these composites.[3]

Specimens, 25-mm-diam by 25-mm-long were tested in compression at 2970 K and 2000 psi (13.7 MPa) for 30 minutes for single point deformation and tested for cummulative deformation by incrementally increasing temperature in 200 K increments from 2270 to 2970 K and measuring deformation. Figure 8 dramatically illustrates minimum deformation of the solid solution composites, and Figure 9 illustrates the strong effect of iron impurity concentration in the niobium carbide powder on deformation of the hot pressed composite.

The bank of ten high temperature hot presses used for composite component production for the reactors is shown in Figure 10. We made most of the pressings at ~ 3320 K and 3200 psi (22 MPa), maintaining these maximum conditions for ten minutes. Figure 11 shows the

various shapes required and the graphite dies used to make the right cylinder blanks for these shapes.

4. Heat Shields for Fuel Element Supports

The hot end fuel element support blocks of Phoebus type reactors accommodated button structured tie rods which received the load of the core and transmitted it to the cold end support plates. For the more advanced reactor designs which called for cyclic operation at higher temperatures and longer running times, it was necessary to thermally shield the button tie rod ends with cup and threaded cap type shields. Figure 12 shows the shields and method of manufacture.

Results of preliminary tests under designed cyclic operational conditions indicated that W-Mo-Re and W-Mo alloys would survive without excessive embrittlement or reaction with niobium carbide coated graphite support blocks. We subsequently developed a process using tungsten - 30 wt% molybdenum with 1.5 wt% thoria added for manufacturing these components with minimum material waste and minimum machining time.[4]

We isostatically pressed a blended mixture of ball-milled thoria and fine tungsten and molybdenum powders around mandrels at 45,000 psi (310-MPa). Machine time for fabricating these threaded cap and cup shields to exacting dimensional specifications was reduced to approximately one hour each by performing conventional machining after a 15 h presinter in hydrogen at 1273 K. No further machining was required after the subsequent sintering for 15 h at 1973 K and 1.5 h at 2973 K in flowing hydrogen.

These alloy shields retained their self-supporting characteristics without serious embrittlement and provided the necessary thermal shielding during actual reactor cyclic operation at ~ 2800 K.

II. Thermionic Emitter Reactors

The use of electrical propulsion for advanced space missions is dependent on development of long lifetime, low weight nuclear electrical power supplies. Thermionic reactors with efficient heat-to-electricity conversion taking place in-core can meet the weight restrictions but it was necessary to devleop fuel pins with lifetimes of 10,000 hours operation with a high degree of dimensional stability at elevated temperature in a cesium atmosphere.[5] The cesium acts as a metal coolant to carry away heat at the cold junction and serves as the electrical conductor.[6]

A. Uranium Carbide-Zirconium Carbide Fuel Pins

Calculations indicated that a 30-mole percent uranium carbide - 70 mole percent zirconium carbide (melting point ~ 3200 K) fuel pin operating at 2300 K would have low vapor pressure and adequate emission properties, and that this high temperature would anneal out a considerable portion of fission product damage and promote release of fission products.

Because of compatability problems with the cesium vapor in which the fuel pin operated; trace amounts of free carbon and second phases such as UC_2 or U_2C_3 could not be tolerated in this very reactive material. We investigated many avenues for preparing solid solution powder for hot pressing 6-mm-diam by 125-mm-long fuel pins, the upper 100-mm of which was enriched uranium.[7]

We first made very fine, high purity raw material powders of uranium, uranium hydride, uranium mono-carbide, zirconium, zirconium hydride and zirconium carbide, and then reacted these in various combination to form the solid solution UC·ZrC powder. We also made the solid solution powder by first arc melting 100 gram buttons of uranium, zirconium and carbon which we homogenized for 24 h at 2000°C in vacuum. We then crushed the buttons -200 mesh, homogenized the powder for an additional 24 h and ball milled it in a uranium ball mill with uranium balls.

We made high density fuel pins by vacuum hot pressing [at 2470 K and 4400 psi (30.3-MPa)] carefully weighed and leveled charges of enriched powder loaded on top of depleted solid solution carbide powder. Figure 13 (626035) shows the pins and the five-hole graphite die assembly for making the pins. A hole was drilled through the pin for venting fission products.

It was subsequently determined that the brittle character of the carbide when subjected to radiation, thermal and mechanical shock, and vibration, and its incompatability with refractory metals which it contacted, required abandoning UC-ZrC as a fuel pin.

B. Molybdenum-Uranium Oxide Fuel Pins

A molybdenum -40 volume percent enriched uranium oxide fuel pin coated with 0.12-mm of tungsten was designed for 10,000 hour operation at 2100 K. Because fission product escape is governed by diffusion from the UO_2 particles in the cermet and hence is critically dependent on particle size as well as on the temperature, we had to carefully select molybdenum and oxide powders with specific characteristics so that we could fabricate fuel pins to accommodate fission gas release and prevent pin swelling. Introducing porosity in the cermet and

drilling a hole in the center of the fuel pin were effective in minimizing pin swelling but it was also necessary to have a relatively high density metal matrix to minimize oxide migration.

We isostatically pressed 105 micron diam oxide particles with fine molybdenum and sintered the pressings at 2000 K, or hot pressed the powders to form products with 8 to 12 percent open porosity. We then heated the material to ~ 2400 K in vacuum to stabilize the porous structure to prevent additional sintering at the long time, but lower temperature operation.[8]

Fuel pins were machined to size and coated with tungsten from the hexafluoride. Irradiation tests under reactor conditions for 8068 hours produced only one percent swelling of the fuel pins, and it was concluded that these fuel pins could operate satisfactorily for this extended life at 2100 K. Post irradiation test examination of the fuel pins led to the conclusion that even longer life operation could be achieved by introducing more initial porosity in the pins.

III. Laser and Electron Beam Fusion Programs

A. Lithium Deuteride-Tritide Targets

Our laboratory is engaged in experimental and theoretical efforts based on the concept of initiating thermonuclear fusion reactions by concentrating pulsed laser energy on small pellets of deuterium-tritium fuel. One objective of the laser program was the study of energy interaction of a laser beam with lithium deuteride or lithium deuteride-tritide (LiDT), and calculations indicated maximum deuterium-tritium burn efficiency using a spherical 100-μm-diam LiDT particle.[9]

Lithium deuteride is a very reactive material; large lumps can be briefly handled in air but finely divided powder with its high surface area and low thermal conductivity reacts instantly with small amounts of water or water vapor, sometimes with explosive violence, and the liberated hydrogen ignites spontaneously. Therefore, all operations with powder were performed in a very dry argon atmosphere.

Five processes for preparing spherical powders were investigated briefly using lithium hydride as a stand-in for lithium deuteride:

1. Spheriodization and hydriding of metallic lithium in non-reactive oil.
2. High pressure atomization of molten lithium hydride.
3. Discharge of molten lithium hydride thorugh a perforated plate.
4. High pressure extrusion of 100-μm-diam rod with subsequent sperhoidization of chopped rod.
5. Gravity flow of powder through a heated drop tower.

We used the last technique to produce lithium deuteride spheres for laser targets. This technique consists of dropping angular lithium deuteride particles at a controlled rate vertically through a hot zone where they melt to form spheres that cool and solidify while falling free. One of the drop towers used successfully is shown in Figure 14.

We hand crushed large irregular lumps of deuteride in an argon atmosphere glove box to yield a 95 to 140 micron size angular powder as shown in Figure 15. We made many spheroidizing runs varying length of the hot zone and temperature of hot zone, and found a temperature range of 1098 to 1123 K and a hot zone length of ~ 90-mm

to be optimum for producing an acceptable yield of good solid spheres as shown in Figure 16. In this temperature range we were able to affect only surface melting and thus prevent shrinkage voids which result from complete particle melting.

We were able by a special repetitive screening and cleaning operation to remove the very small dust particles of deuteride from the surfaces of the angular feed powder to obtain a cleaner powder as shown in Figure 17; we obtained smoother surface spheres with the clean powder feed.[10]

We shape classified spheroidized lithium deuteride powder on an adjustable inclined vibratory table to separate spherical from non-spherical powders, and were able with two passes on the table to remove ~ 98% of non-spherical particles.

Of major importance is the deuterium content of the particles; the high dissociation pressure at spheroidization temperature reduced the deuterium content approximately 20 percent. We determined that we could restore most of the deuterium lost by thermally cycling the spheres in purified deuterium between 598 and 773 K using twelve cycles in a 13 h period.

We believe that an isotopic exchange using tritium instead of deuterium will be most favorable for production of lithium deuteride-tritide spheres at the stage where the powder is considerably sub-stoichiometric.

We used a low power microscope to examine and select individual sized and redeuterided particles, and examined them by microradiography at 3 or 4 equatorial planes, or by optical examination with a laser interferometer to determine acceptability as targets.

We then coated the spheres with a thin coating of aluminum or nickel which both protected the particles so they could be handled in air, and acted as a pusher to enhance energy coupling with the laser.

B. Gas Filled Glass and Metal Microballoons

We are currently using miniature (100-600-μm-diam) pressure vessels filled with deuterium-tritium gas targets for both laser and electron beam fusion programs. These vessels are constructed of thin wall glass or nickel alloy microballoons over coated with nickel.

These microballoons are produced commercially for much less demanding applications and contain a high percentage of malformed, pin-holed or broken balloons, and balloons with non-uniform wall thickness or other wall or surface defects. Figure 18 shows a "high-quality" lot of as-produced metal microballoons; as-received glass microballoons were similar but smaller.

We had to classify very large quantities of these very fragile balloons into narrow size fractions, and quality upgrade them to provide a small number of uniform wall, nearly sperhical balloons without significant surface defects. We found that most conventional powder screening equipment damaged a rather high percentage of these fragile balloons, and additionally, their low density and electrostatic attractive forces prohibited obtaining sharp, narrow size classification with this equipment.

We initially floated balloons in ethanol with gentle stirring to affect a gross separation of sinkers and floaters. Screening through an inverted stack of sieves agitated in an ultrasonic cleaner filled with ethanol, effectively overcame the attractive

forces and permitted accurate sizing. We also used the device shown in Figure 19 to float particles up through screens for sizing.

We subsequently eliminated most of the sized but weak wall or holey balloons by alternately evacuating and opening to the atmosphere, a pentane filled flask shown in Figure 20 which allowed the broken or defective balloons to sink to the bottom and be withdrawn.

In addition to the batch sizing and quality upgrading, we developed methods for classification of individual balloons according to size, shape, and surface quality at a rate of 25-to 40-per hour using a 30 power stereo microscope. After multiple viewing and rotating selected balloons, we mounted them in regular arrays and radiographed at a minimum of two equatorial planes. Prints of radiographs were enlarged and the wall thickness uniformity, diameter, and sphericity determined. Figure 21 shows a radiograph of coated metal microballoons and demonstrates usefulness of this technique for inspection.

IV. Current Programs

We very recently hot pressed hercynite-hematite for the joint US-USSR (Soviet) MHD program. We are currently engaged in more conventional powder metallurgy work including 1) forming shapes of tungsten alloy by plasma-arc-spraying and by cold pressing and sintering prealloyed powder 2) plasma-arc-spraying a wide variety of powders to form high density shapes 3) fabricating controlled porosity structures by hot pressing (or cold pressing and sintering) a combination of powders and screen (or fibers) 4) preparation of high purity minerals in powder form and hot pressing the powders to nearly theoretical density for the geosciences and geochemical community and for equation-of-state-studies, 5) preparation of specimens of

niobium-aluminum-germanium for use in superconductivity studies.

We also recently began investigating hot pressing and hot isostatic pressing of $CoCr_2S_4$ for use as Faraday rotators for laser beam application.

References

1. D. H. Schell, "Fabrication of Fuel Elements for Kiwi-A Reactor," Los Alamos Scientific Laboratory report LA-2418, 1960.

2. H. Sheinberg and R. W. Keil, "Fabrication and Properties of Copper-Boron Carbide Control Materials for Phoebus II Reactor," Transactions of American Nuclear Society, 9, [1], (1966).

3. K. V. Davidson, R. E. Riley, and J. M. Taub, "Carbide Graphite Composites," Second Progress Report, Los Alamos Scientific Laboratory report number LA-3652-MS, 1967.

4. R. E. Riley and C. E. Landahl, "High Temperature Protective Heat Shield," Los Alamos Scientific Laboratory report number LA-3950, 1968.

5. W. A. Ranken, "Second Status Report on High Temperature Irradiation of Mo-UO_2 Fuel," Los Alamos Scientific Laboratory report number LA-3462, 1966.

6. "Quarterly Status Report of the Los Alamos Scientific Laboratory Plasma Thermocouple Development Program," for the period ending November 20, 1964, Los Alamos Scientific Laboratory report number LA-3195-MS.

7. K. V. Davidson, R. E. Riley, and J. M. Taub, "Solid Solution Carbides of Uranium and Zirconium," Los Alamos Scientific Laboratory report number LA-3217, 1965.

8. "Quarterly Status Report of the Los Alamos Scientific Laboratory Plasma Thermocouple Development Program," for the period ending July 20, 1964, Los Alamos Scientific Laboratory report LA-3128-MS.

9. H. Sheinberg, R. E. Riley, and J. M. Taub, "Spheroidization and Coating of Lithium Deuteride," Los Alamos Scientific Laboratory report number LA-4905-MS, 1972.

10. D. H. W. Carstens, E. H. Farnum, R. J. Fries, and H. Sheinberg, "Fabrication of $LiD_{0.5}T_{0.5}$ Microspheres for Use as Laser Fusion Targets," Journal of Nuclear Materials, 57, 1-10 (1975).

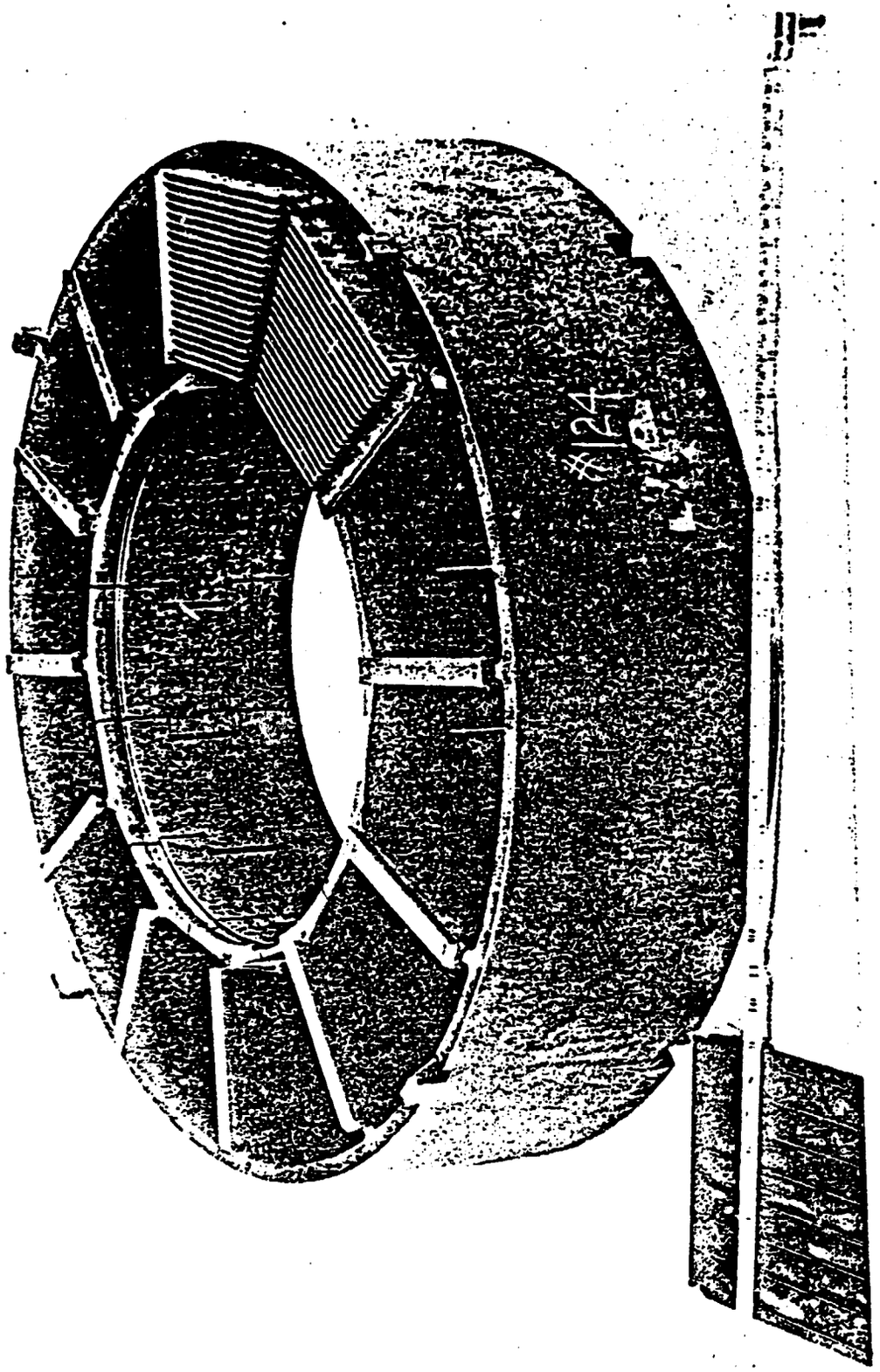

Figure 1 Graphite whim partially loaded with fuel element plates.

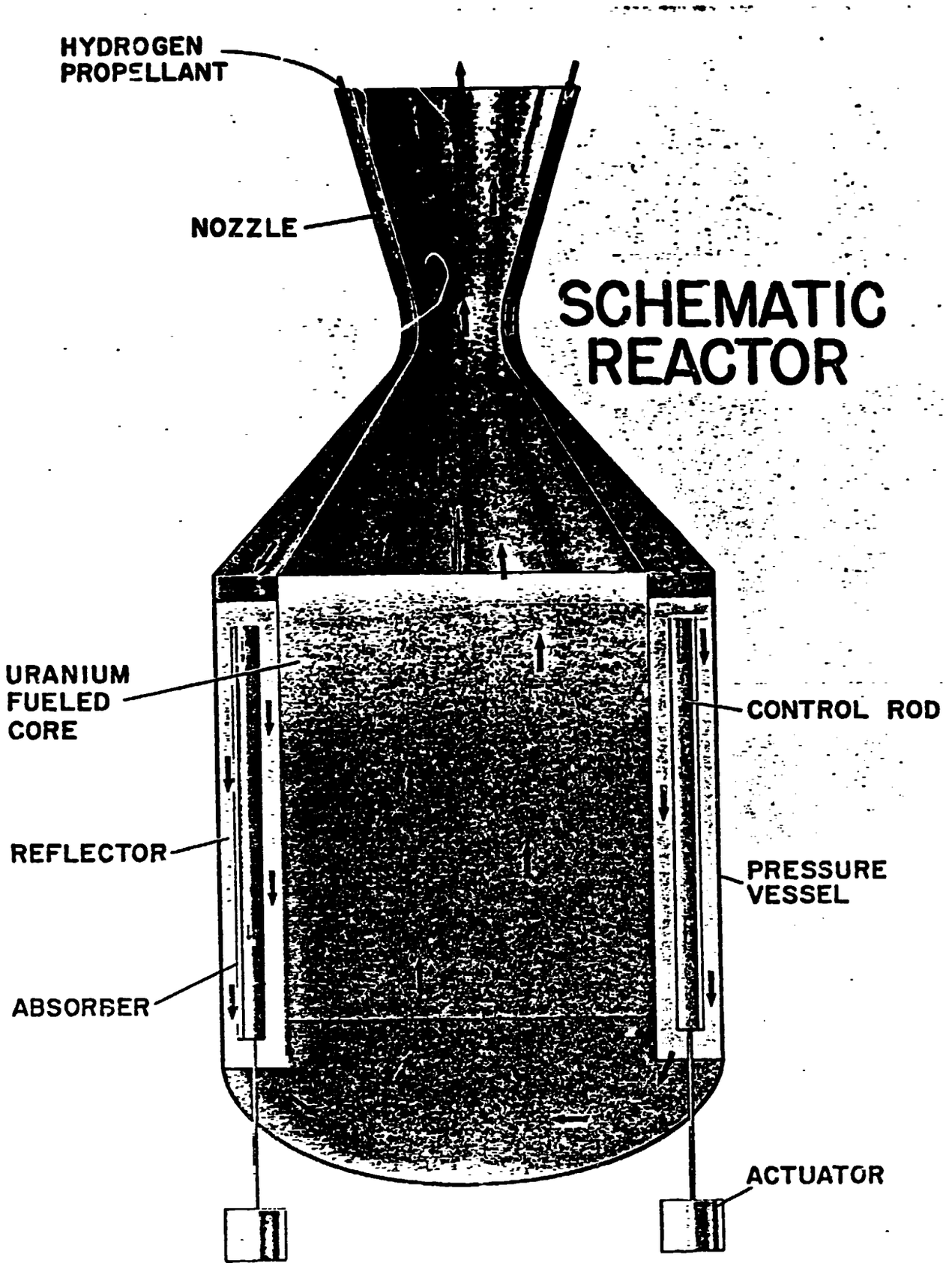

Figure 2. Phoebus Type Rocket Propulsion Engine.

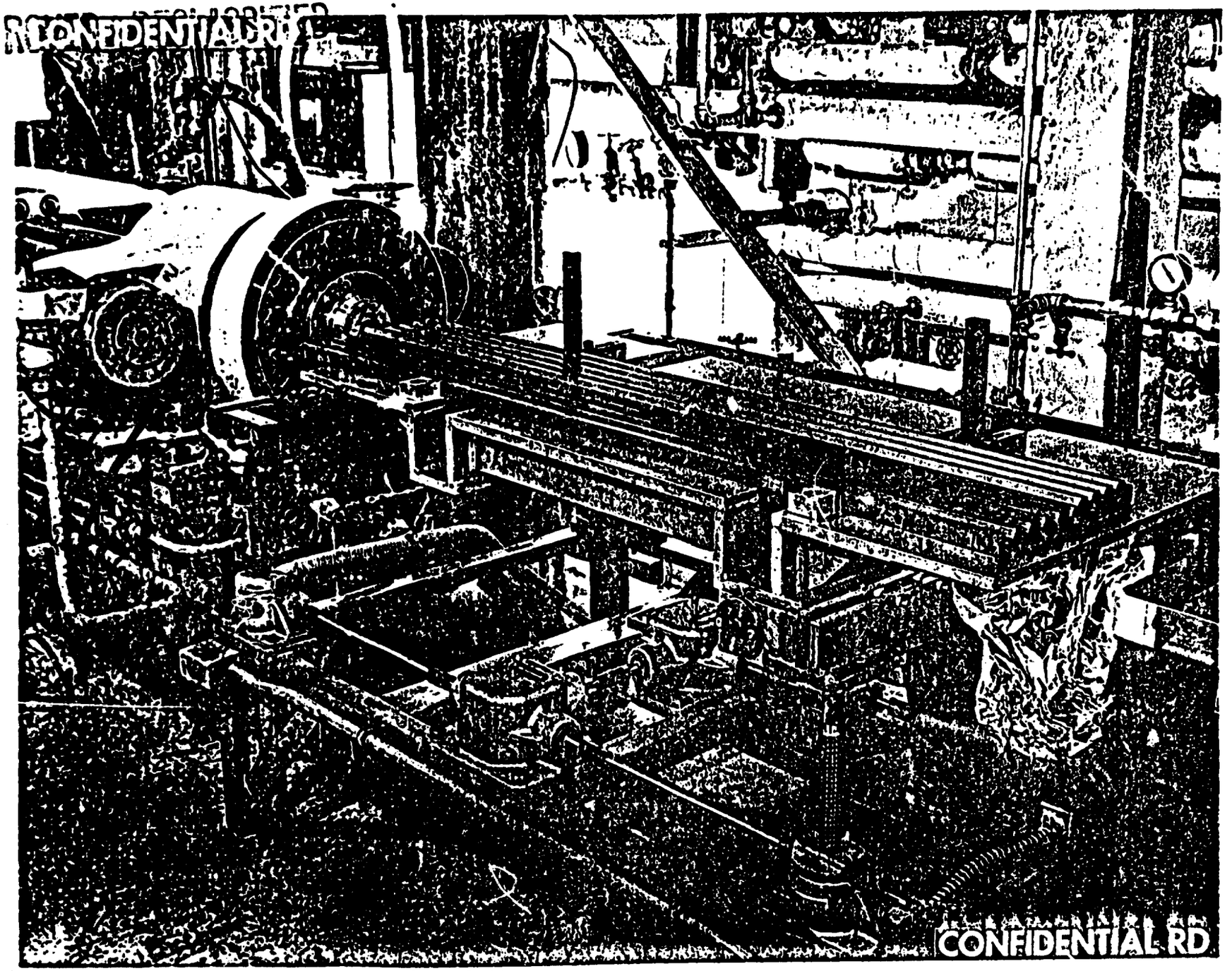

Figure 3. Extruded 19 Hole Hexagonal Fuel Elements.

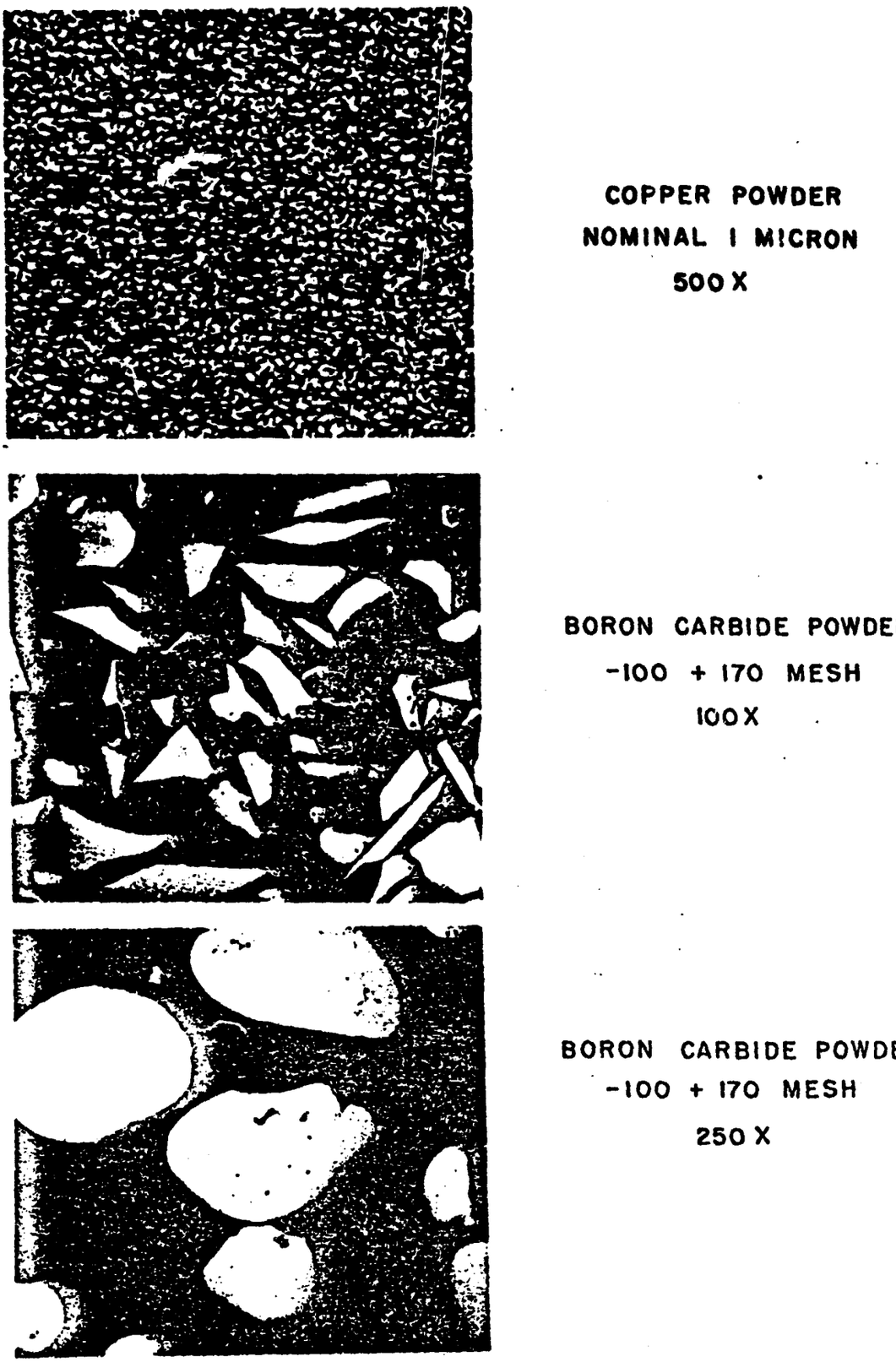

Figure 4. Raw Materials for Control Plates.

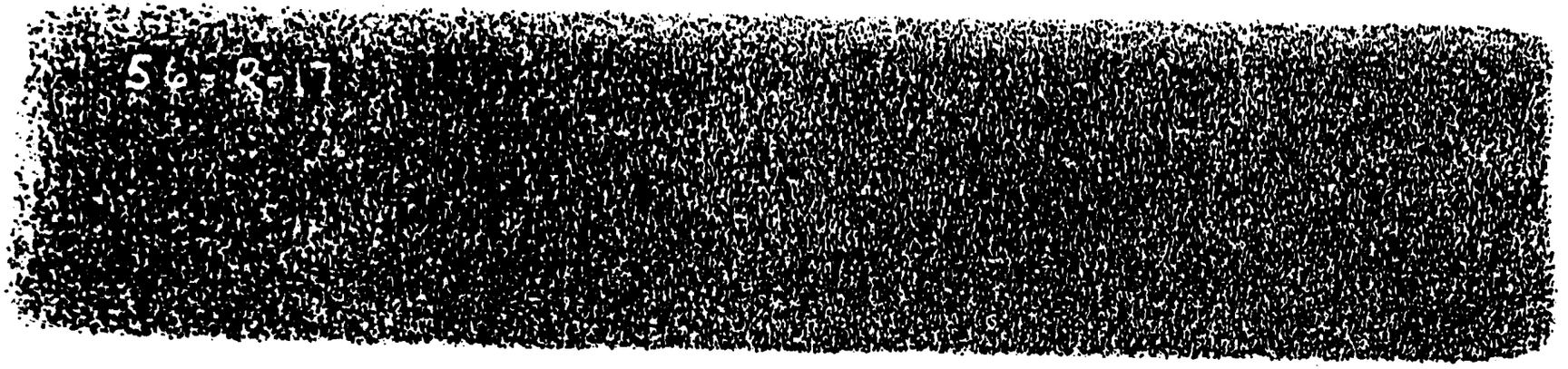
56-R17

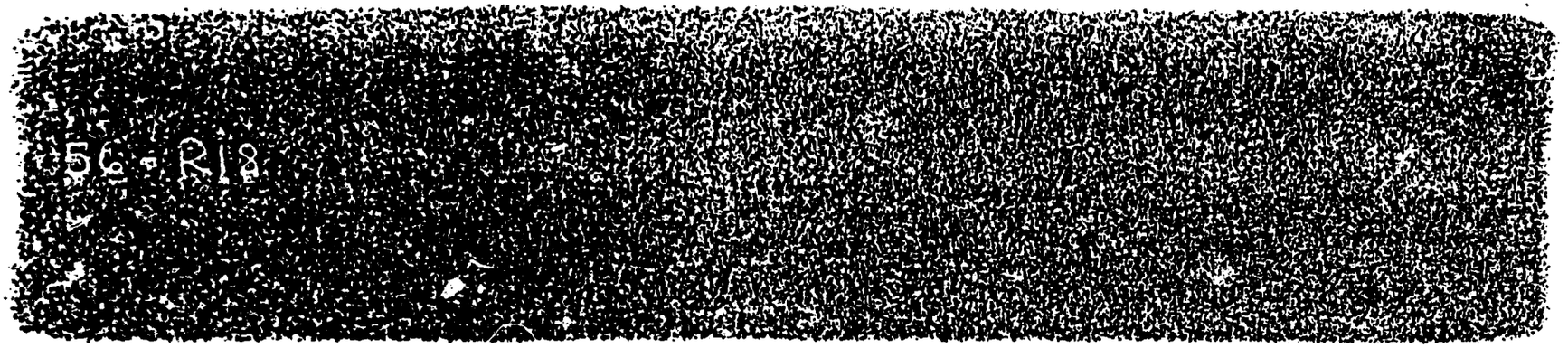
56-R18

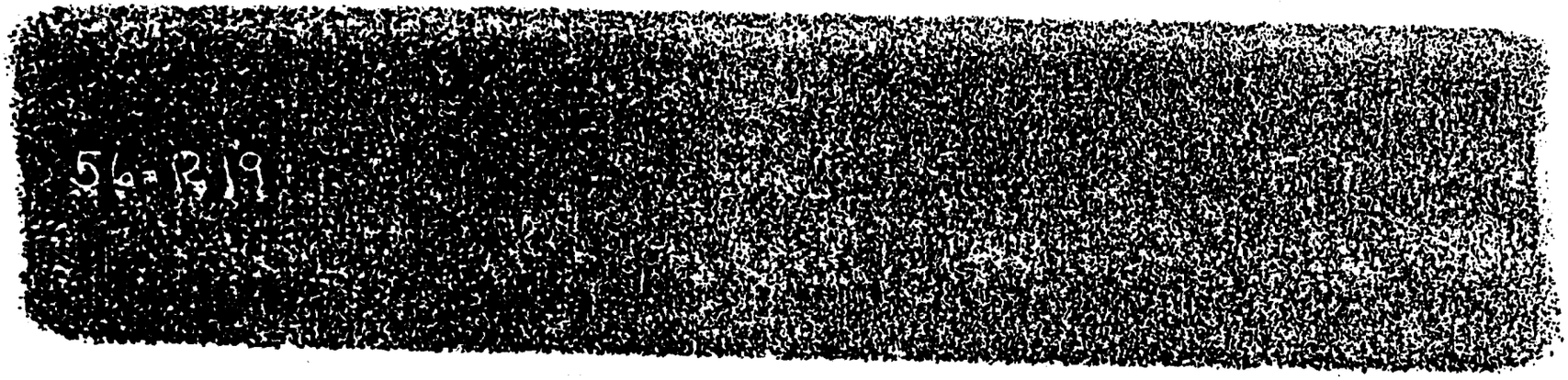
56-R19

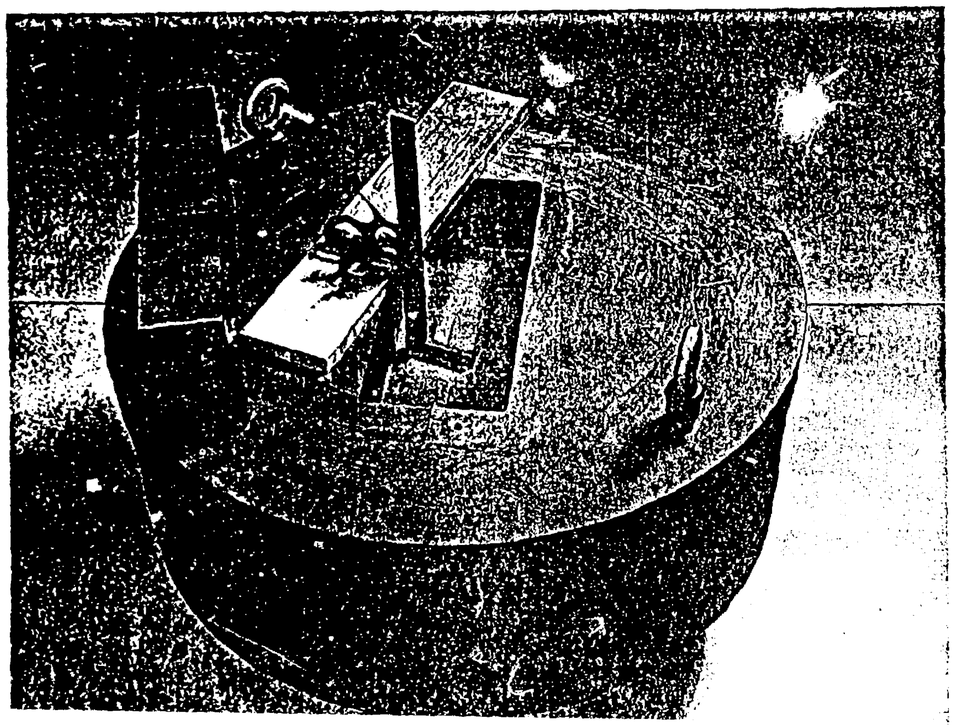

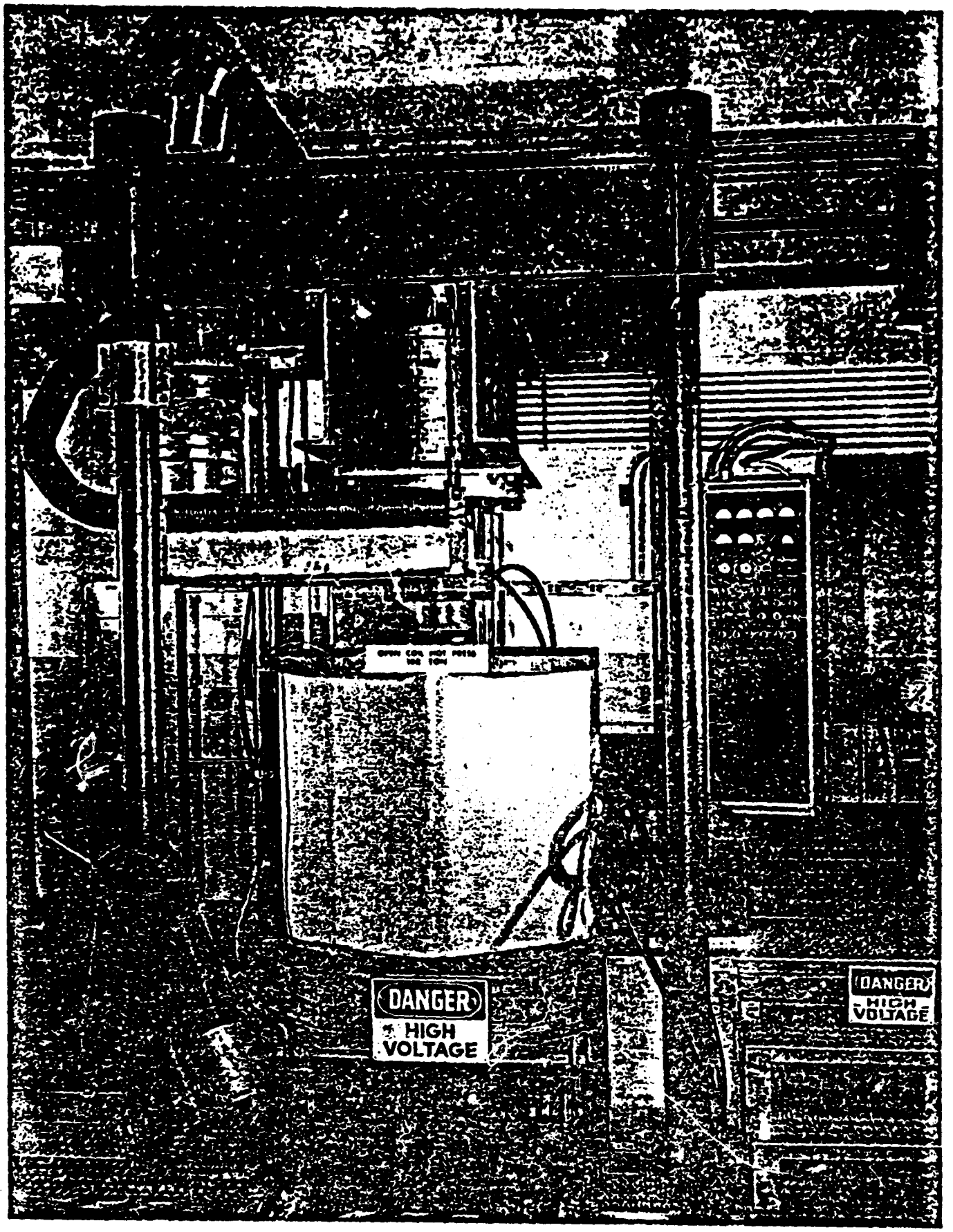

Figure 7. 100 Ton Capacity Hot Press.

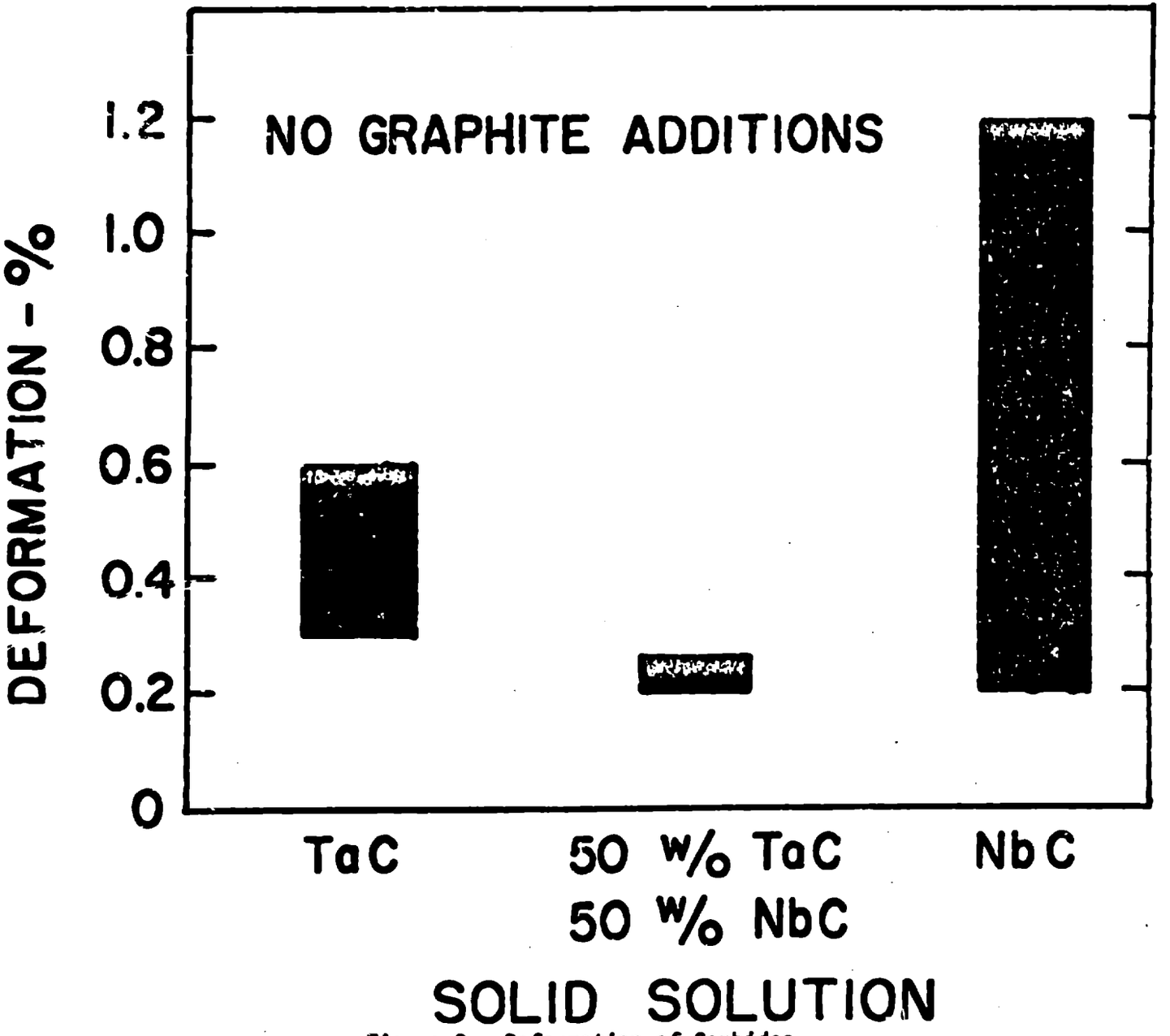

Figure 8. Deformation of Carbides.

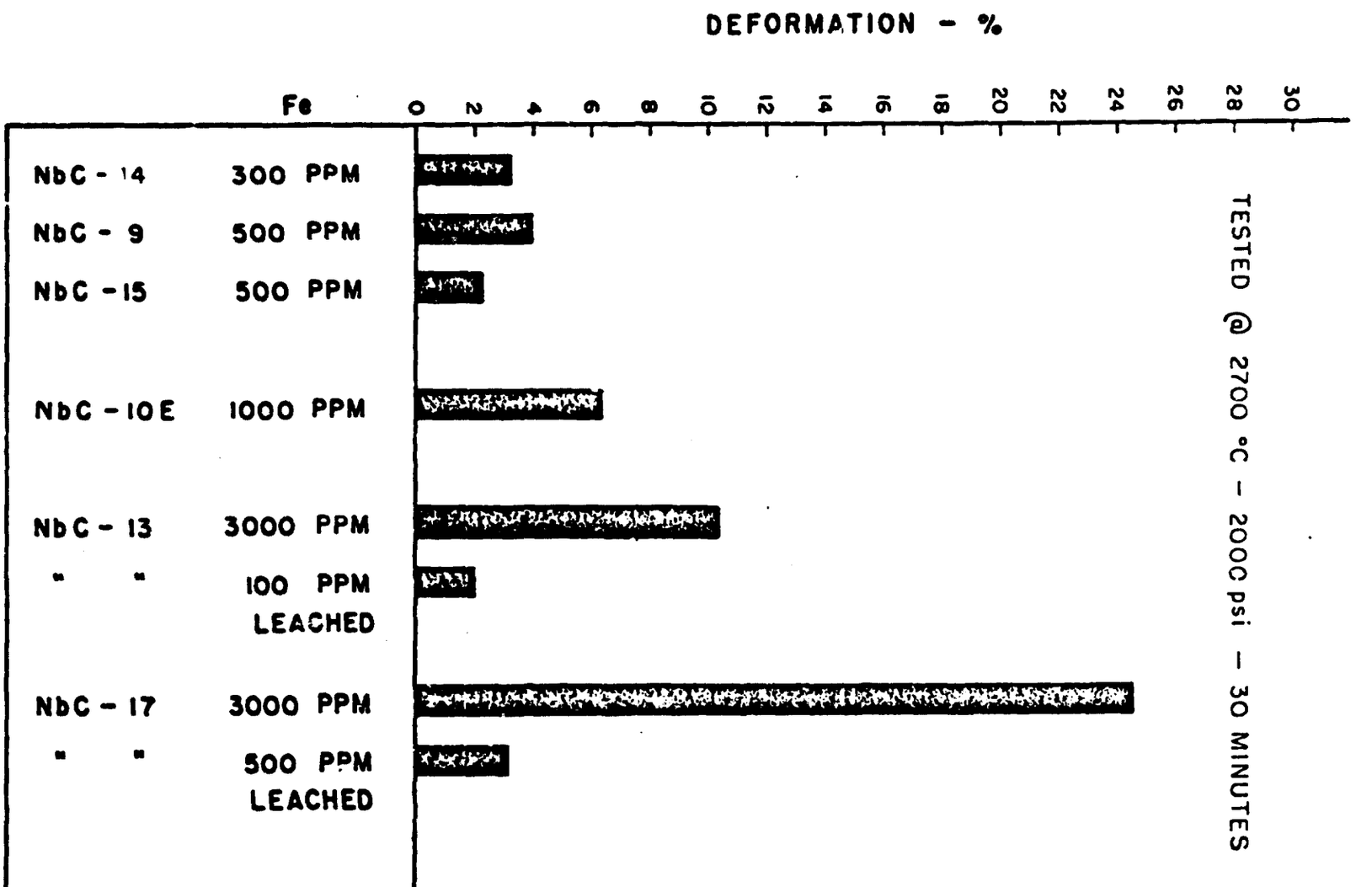

Figure 9. Effect of Iron Impurity on Deformation.

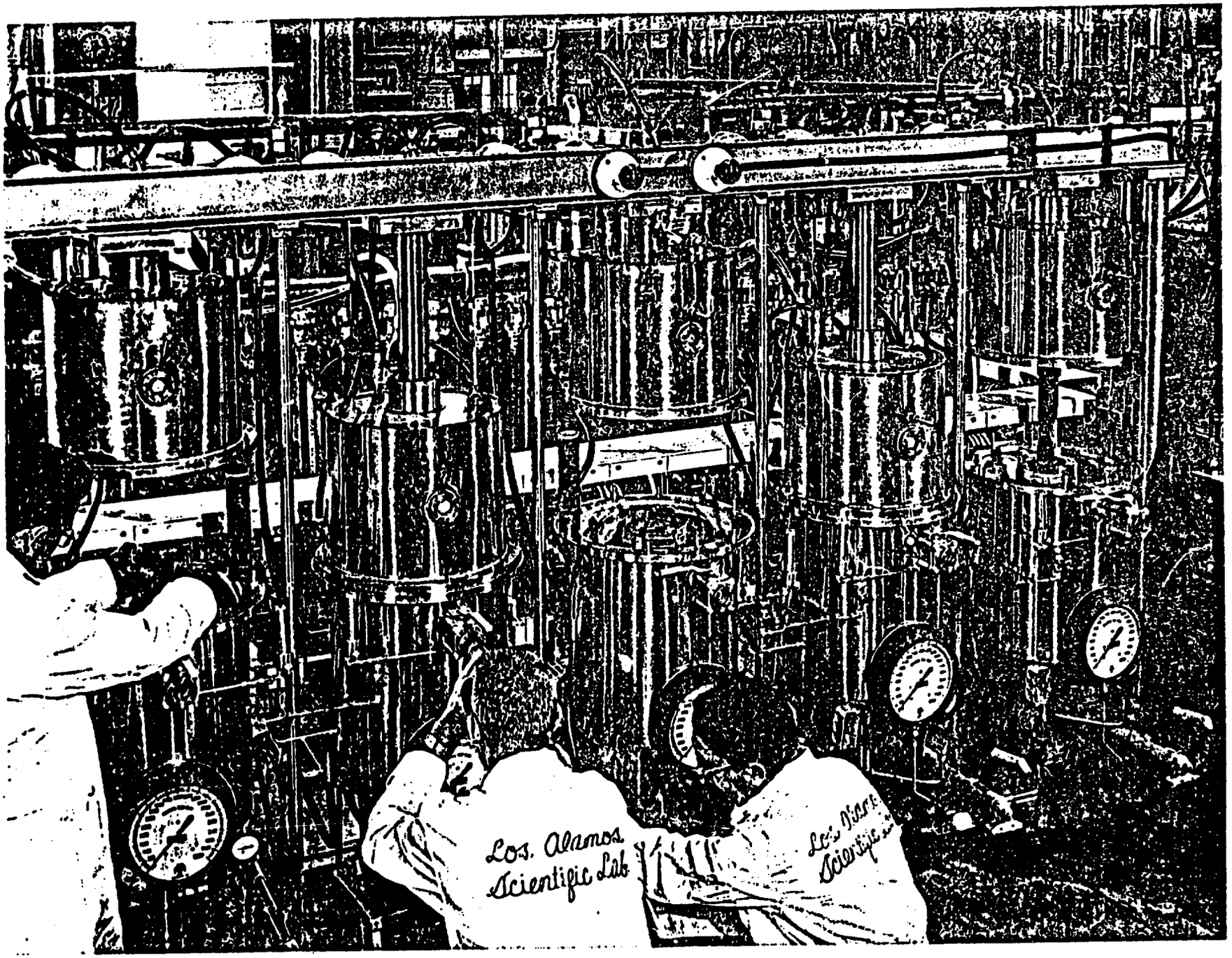

Figure 10. Argon Atmosphere High Temperature Hot Presses.

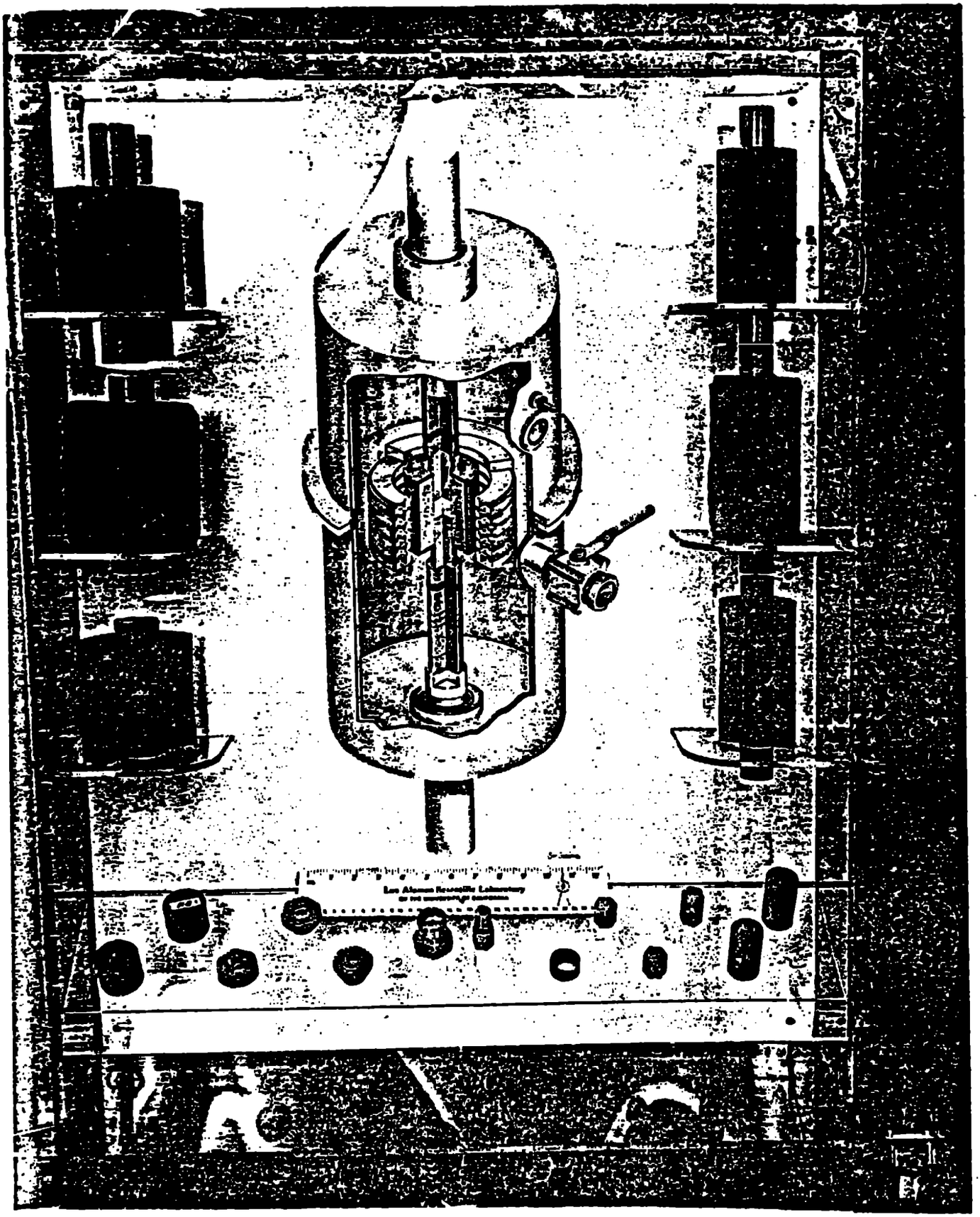

Figure 11. Hot Press Construction, Dies and Hot Pressed Shapes.

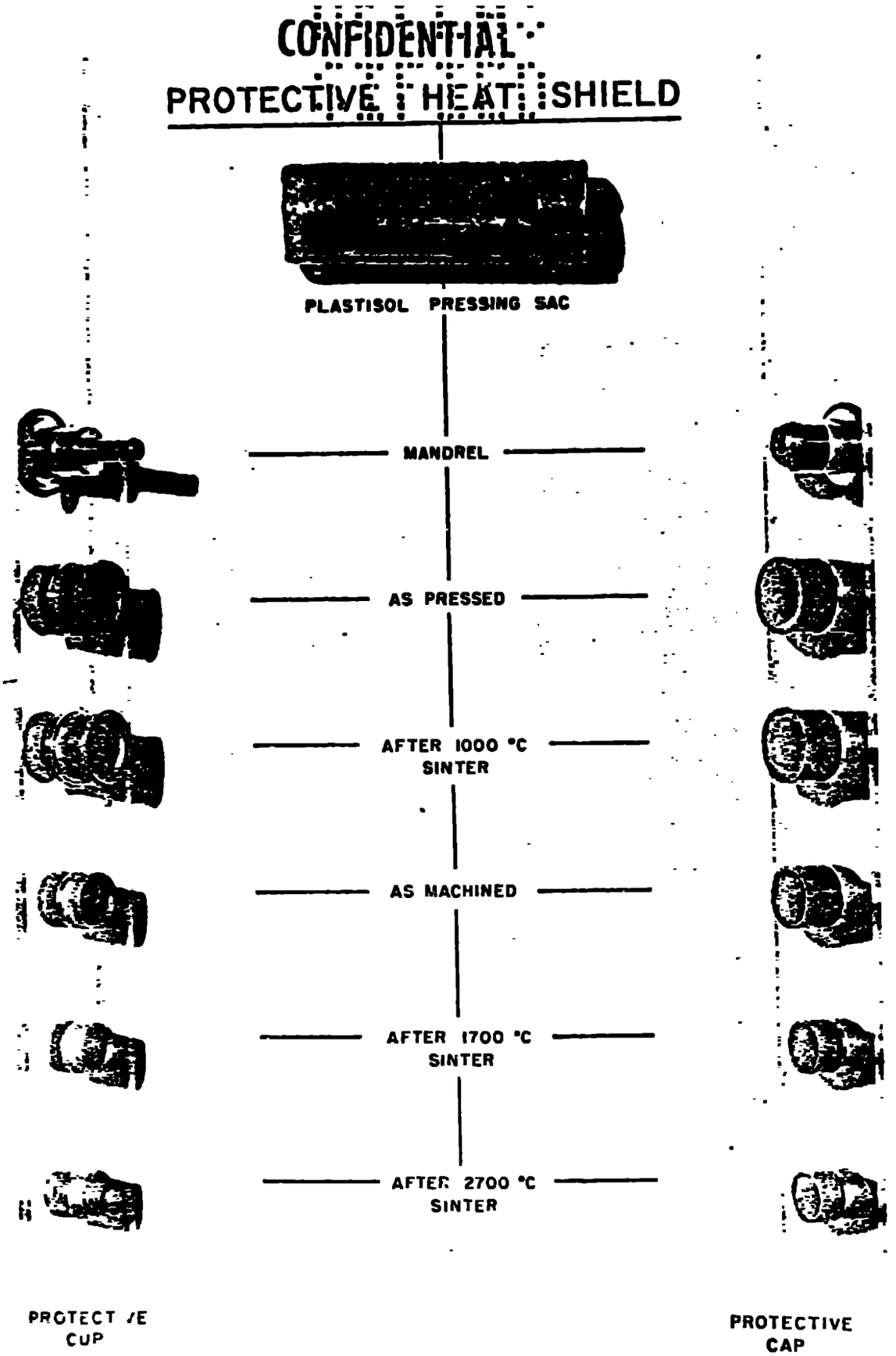

Fig. 2. Manufacturing steps for protective heat shield components.

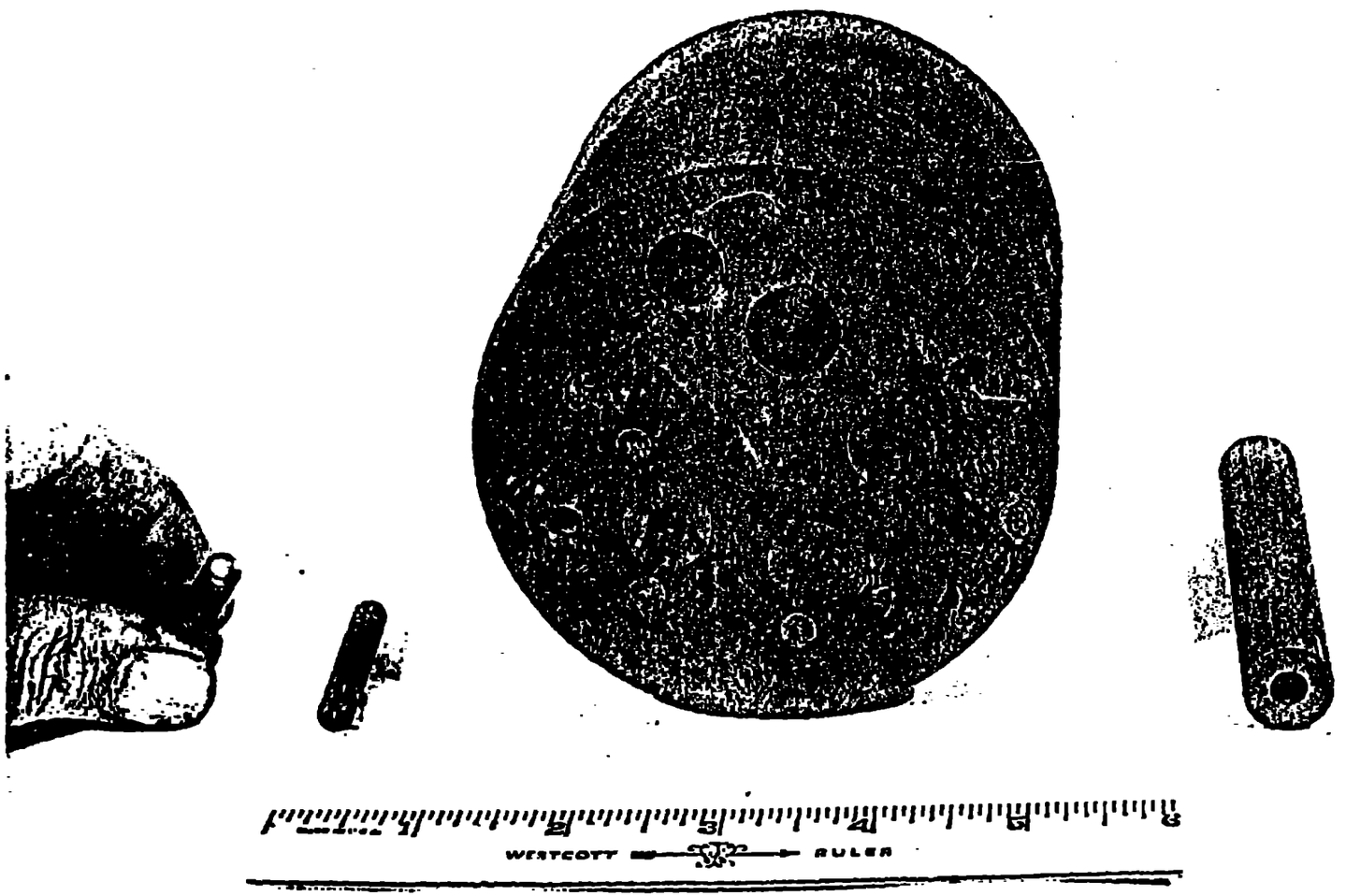

Figure 13. Die Assembly and Hot Pressed Carbide Fuel Pins.

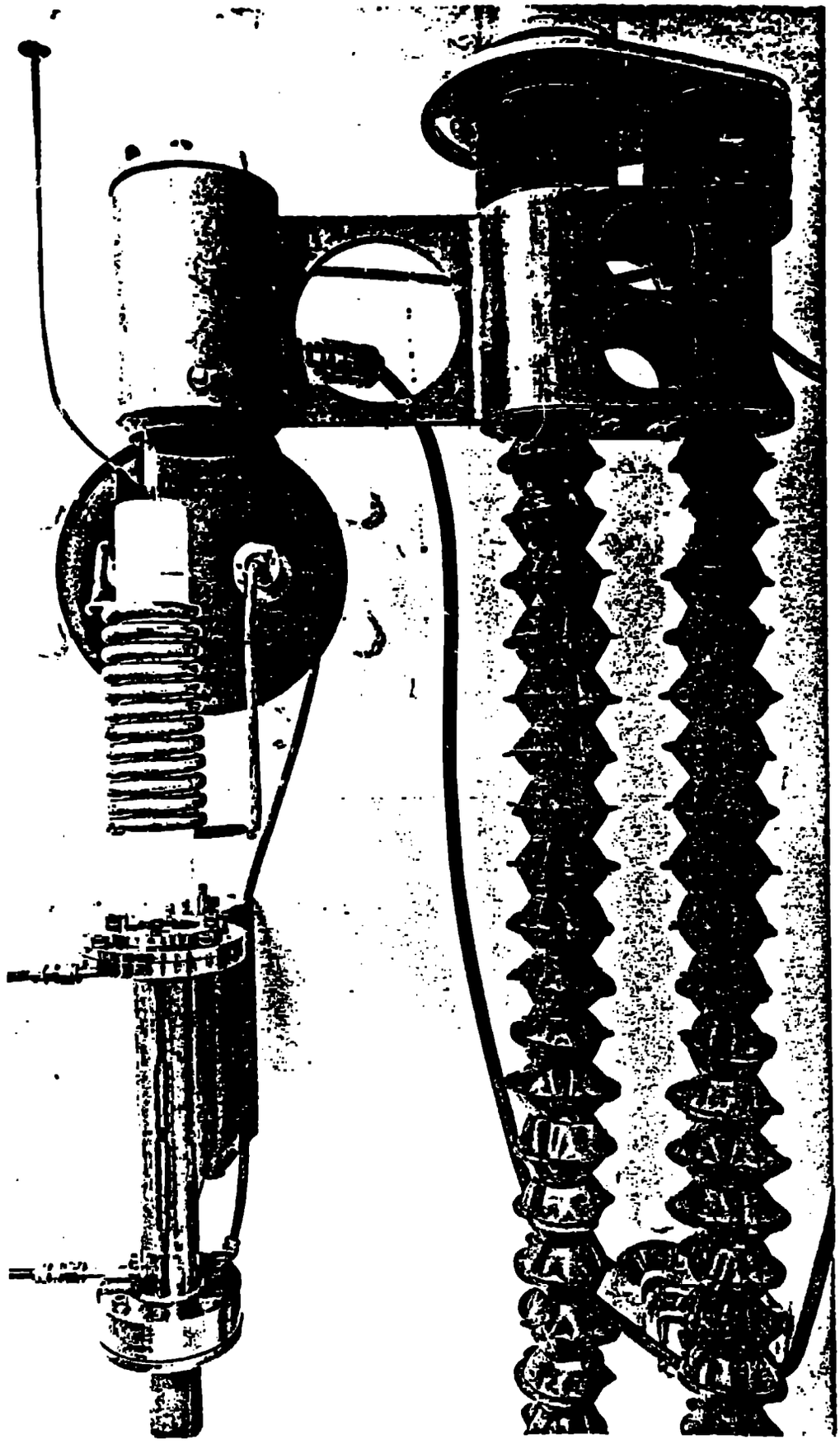

Figure 14. Drop Tower for Spheroidizing Lithium Deuteride.

Scanning Electron Micrographs
Sample #LiD-1, 1150

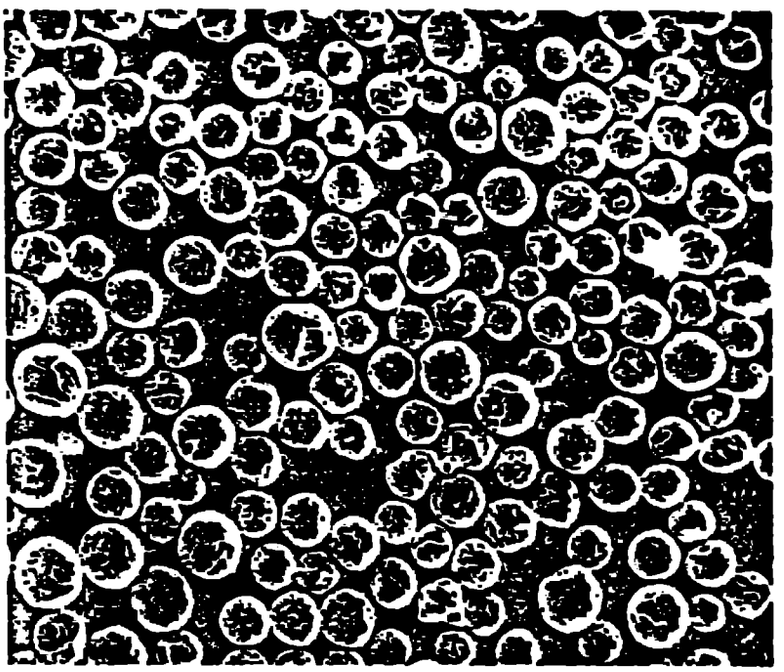

50X

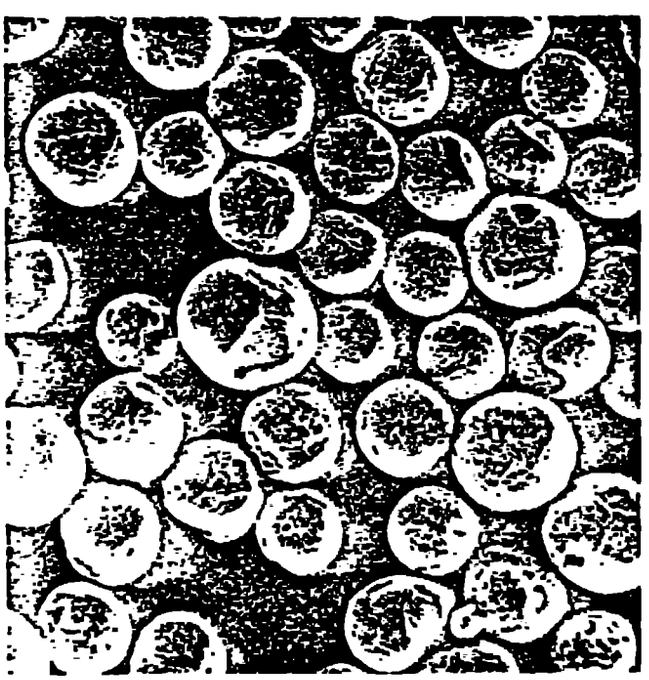

100X

300X

Figure 16. Spheroidized Lithium Deuteride.

Scanning Electron Micrographs
Sample #LiD-2

50X

100X

300X

Figure 15. Crushed and Screened Lithium Deuteride Feed Powder.

Scanning Electron Micrographs
Sample #LiD-4

100X

300X

300X

Figure 17. Special Screened and Cleaned Lithium Deuteride Feed Powder.

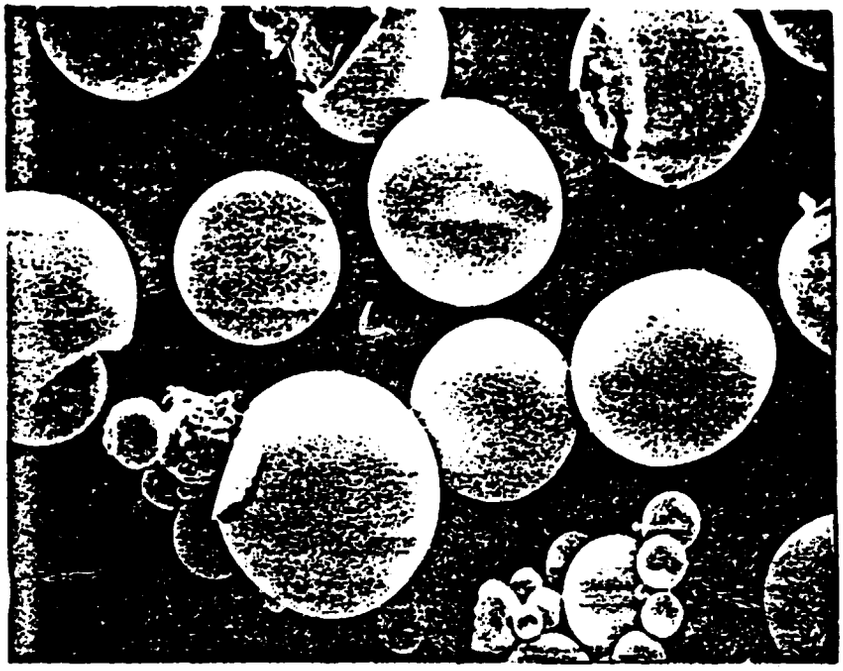

Surface of macroballoons

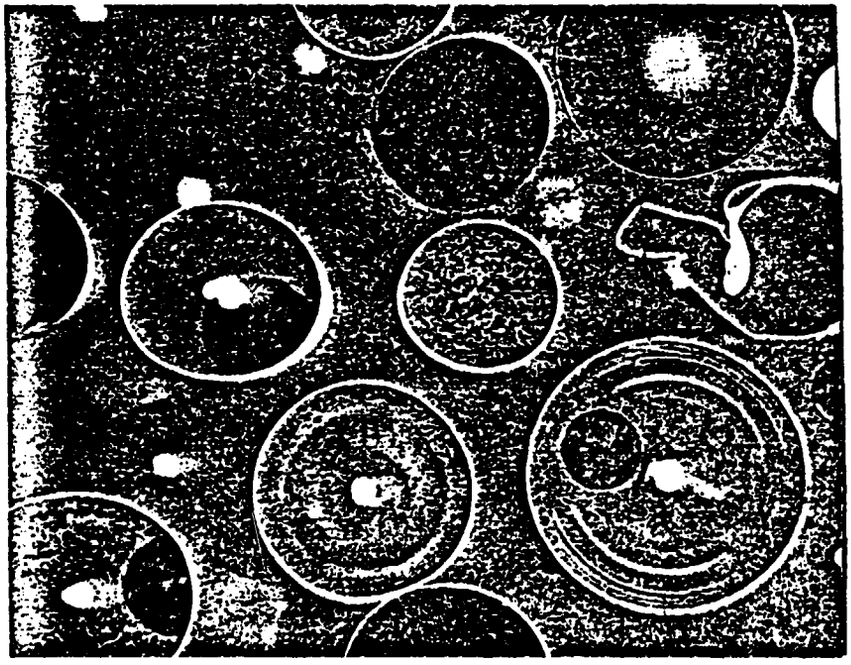

Structure of macroballoons

Figure 18 Surface and structure of as received metal macroballoons, 250X

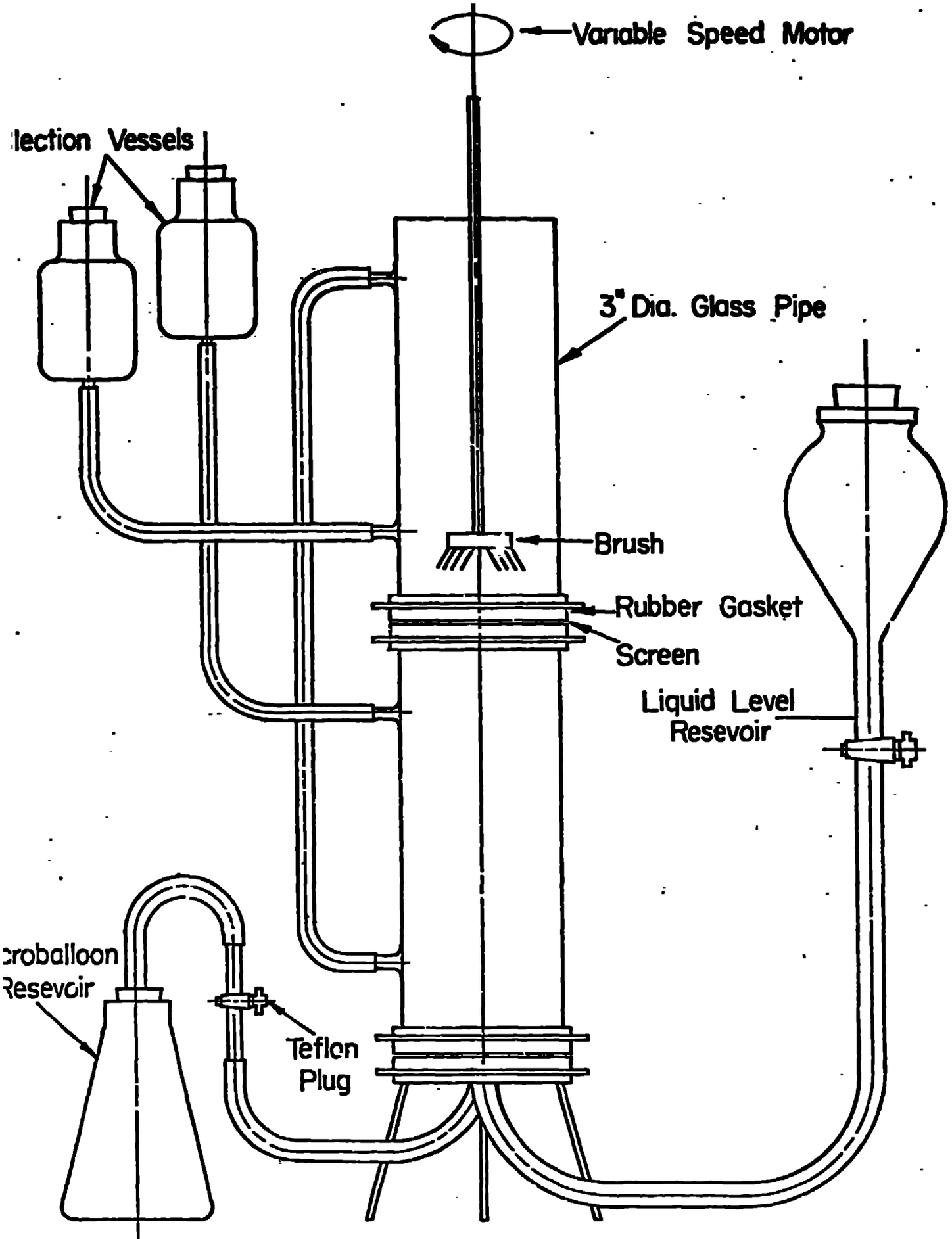

Figure 19. Glass Pipe Liquid Separator

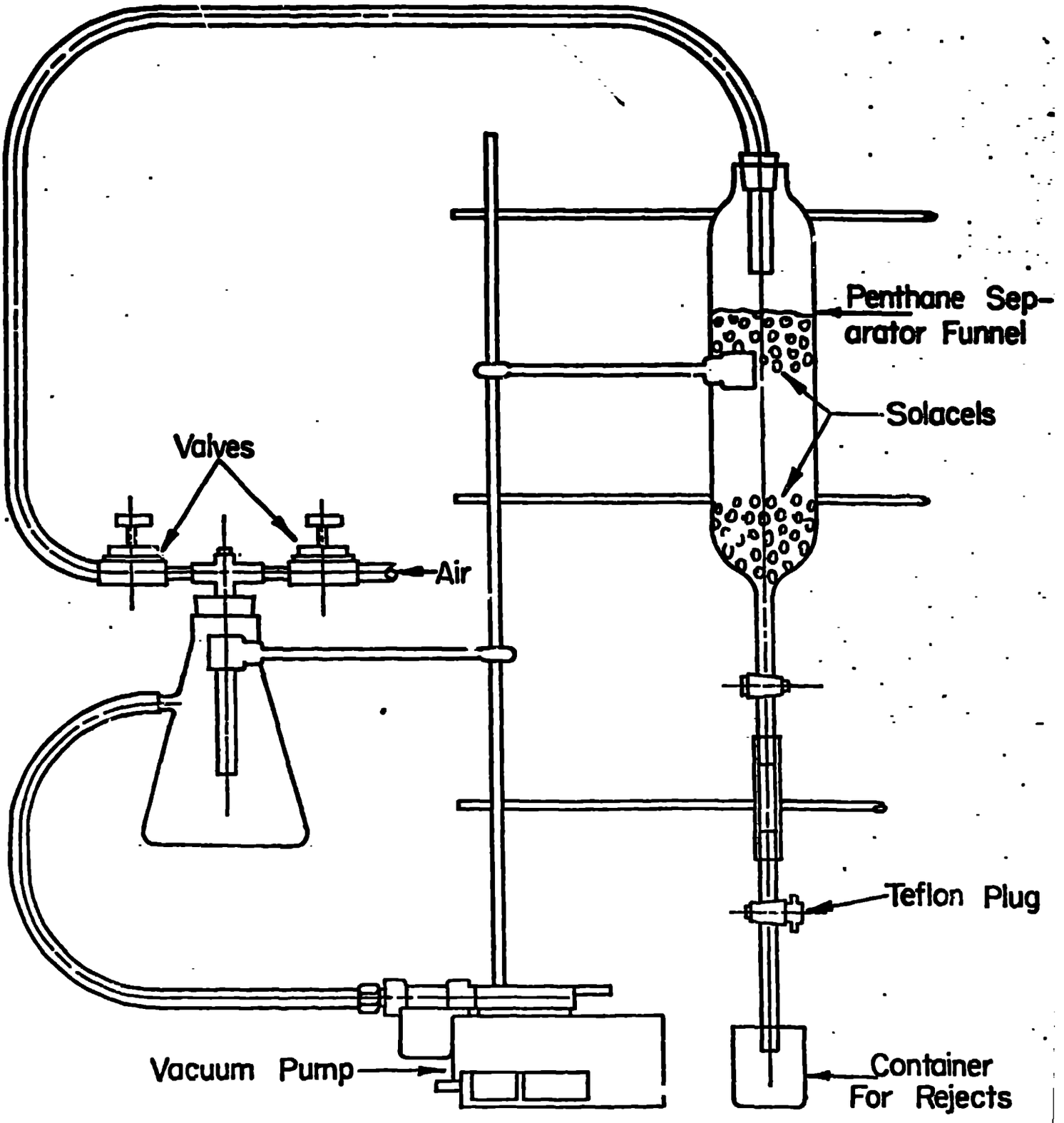

Figure 20. Pentane Floating Apparatus

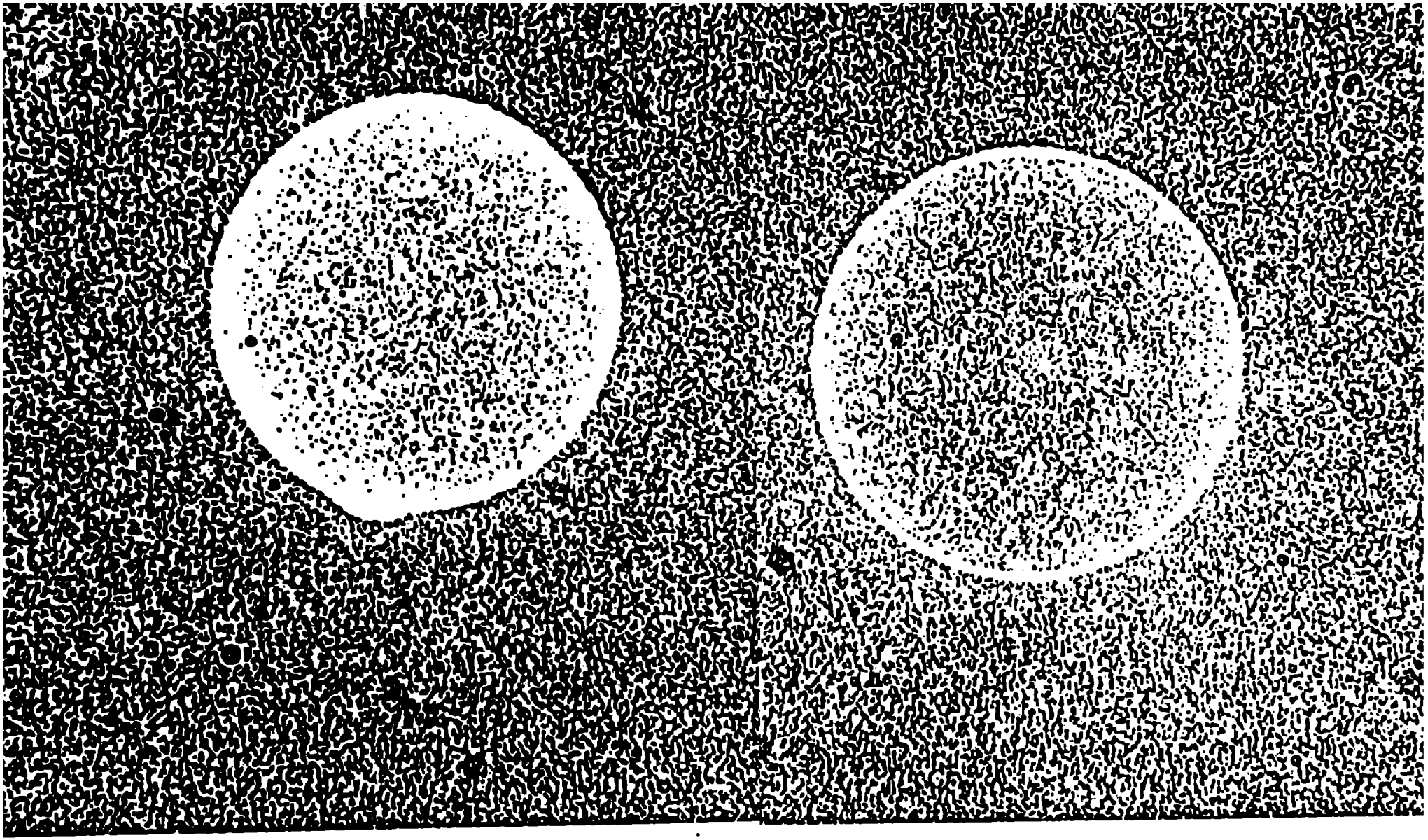

Figure 21. Radiograph of Metal Microballoons.